LTB4 causes macrophage–mediated inflammation and directly induces insulin resistance in obesity

Pingping Li[#1,3], **Da Young Oh**[#1], **Gautam Bandyopadhyay**[1], **William S. Lagakos**[1], **Saswata Talukdar**[1], **Olivia Osborn**[1], **Andrew Johnson**[1], **Heekyung Chung**[1], **Michael Maris**[1], **Jachelle M. Ofrecio**[1], **Sayaka Taguchi**[1], **Min Lu**[1], and **Jerrold M. Olefsky**[1,3]

[1]Division of Endocrinology & Metabolism, Department of Medicine, University of California, San Diego, 9500 Gilman Drive, La Jolla, CA, USA, 92093

[#] These authors contributed equally to this work.

Abstract

Chronic inflammation is a key component of obesity–induced insulin resistance and plays a central role in metabolic disease. In this study, we found that the major insulin target tissues, liver, muscle and adipose tissue exhibit increased levels of the chemotactic eicosanoid LTB4 in obese high fat diet (HFD) mice compared to lean chow fed mice. Inhibition of the LTB4 receptor, Ltb4r1, through either genetic or pharmacologic loss of function results in an anti–inflammatory phenotype with protection from systemic insulin resistance and hepatic steatosis in the setting of both HFD–induced and genetic obesity. Importantly, *in vitro* treatment with LTB4 directly enhanced macrophage chemotaxis, stimulated inflammatory pathways in macrophages, promoted *de novo* hepatic lipogenesis, decreased insulin stimulated glucose uptake in L6 myocytes, increased gluconeogenesis, and impaired insulin–mediated suppression of hepatic glucose output (HGO) in primary mouse hepatocytes. This was accompanied by decreased insulin stimulated Akt phosphorylation and increased Irs1 and Irs2 serine phosphorylation and all of these events were Gαi and Jnk dependent. Taken together, these observations elucidate a novel role of LTB4/Ltb4r1 in the etiology of insulin resistance in hepatocytes and myocytes, and shows that *in vivo* inhibition of Ltb4r1 leads to robust insulin sensitizing effects.

Keywords

insulin resistance; obesity; inflammation; chemotaxis

[3]Corresponding author: Pingping Li (pili@ucsd.edu) or Jerrold M Olefsky (jolefsky@ucsd.edu) .

Introduction

Insulin resistance is a characteristic feature of patients with type 2 diabetes mellitus[1–4]. Obesity is the major cause of insulin resistance, and the current obesity epidemic in westernized countries is driving the parallel type 2 diabetes epidemic. A role for proinflammatory signaling as a cause of insulin resistance was proposed a number of years ago[5,6] and evidence supporting this concept has gradually increased since then[7]. For example, in obesity, there is an increased accumulation of immune cells in the insulin target tissues, adipose tissue[8,9], liver[10], and muscle[11], and this chronic tissue inflammatory state plays a key causal role in obesity–induced insulin resistance[12]. In visceral fat from obese subjects, macrophages can account for 40% of the total cell number and secrete a variety of factors which could impair insulin signaling. In addition, other immune cell types, such as lymphocytes, eosinophils, and neutrophils also contribute to the tissue inflammatory state in obesity[7,13–15].

Leukotriene B_4 (LTB4) is a proinflammatory lipid mediator generated from arachidonic acid through the sequential activities of 5–lipoxygenase, 5–lipoxygenase–activating protein, and leukotriene A_4 hydrolase[16]. LTB4 exerts well–characterized biological actions, including the promotion of leukocyte chemotaxis and the regulation of proinflammatory cytokines by binding to a G protein–coupled receptor termed Ltb4r1 or Ltb4r2[17–19]. Ltb4r1 (also known as Blt1) is the high–affinity receptor specific for LTB4, and is expressed in a variety of inflammatory and immune cells, including granulocytes, eosinophils, macrophages, differentiated Th1, Th2 and Th17 cells, effector CD8 T cells, dendritic cells and osteoclasts. Ltb4r2 (Blt2) is a low–affinity receptor and is expressed more ubiquitously[17–19].

It has reported that the LTB4/Ltb4r1 axis plays an important role in host defense during acute infection. Chronic activation of the LTB4/Ltb4r1 system can also contribute to persistent inflammation characteristic of inflammatory pathologies, including atherosclerosis and arthritis[20–22]. One recent study showed that Ltb4r1 KO mice were protected from inflammation and insulin resistance[23] indicating a role for LTB4 in metabolic dysfunction. In the current study, we report that an Ltb4r1 selective small molecule inhibitor[24–28] markedly reduces tissue inflammation and insulin resistance, both in diet–induced and genetic obese mouse models. Moreover, we unexpectedly found that, apart from its potent pro–inflammatory and chemotactic actions, LTB4 can directly induce decreased insulin sensitivity in myocytes and hepatocytes. All of these findings suggest that Ltb4r1 could be a valuable drug target for the treatment of inflammation and insulin resistance.

Results

Metabolic studies in WT and Ltb4r1 KO or Ltb4r1 inhibitor treated mice

LTB4 is an end product of the leukotriene biosynthetic pathway and working through its unique receptor Ltb4r1, it functions as a potent chemokine promoting migration of macrophages and neutrophils into tissues. We have found that HFD/obese mice exhibit increased levels of LTB4 (2–3 fold) in muscle, liver, and adipose tissue, compared to chow–fed lean mice (Fig. 1a). Based on this, we conducted genetic and pharmacologic loss of function studies to assess the role of the LTB4/Ltb4r1 system in obesity-associated tissue

inflammation and insulin resistance. When place on 60% HFD for 12 weeks, Ltb4r1 KO and WT mice achieved the same degree of obesity (Fig. 1b), while glucose tolerance and hyperinsulinemia were markedly improved in the KO mice (Figs. 1b&c). In addition, the glucose lowering effects of insulin were enhanced in the KO mice (Fig. 1c right panel), indicating an insulin sensitive phenotype. In contrast, there were no effects of the Ltb4r1 KO on glucose metabolism in lean chow–fed mice (Fig. S1). These results in the HFD Ltb4r1 KO mice are fully consistent with the work of Spite *et al*[23].

To further define the role of the LTB4/Ltb4r1 system and to assess its translational potential, we treated male HFD mice with an Ltb4r1 specific inhibitor CP105696[24–28]. This compound is highly selective for Ltb4r1 vs. Ltb4r2[24] and the structure is provided in references 22 and 23. These mice were fed HFD for 14 weeks and then given vehicle or the Ltb4r1 inhibitor (50 mg kg^{-1}) by oral gavage starting at week 12 of HFD. Consistent with the phenotype of the KO mice, treatment with the Ltb4r1 inhibitor markedly improved glucose tolerance (Fig. 1d) as well as the glucose lowering effect of injected insulin (Fig. 1e) without any change in body weight (Fig. 1f left panel). Ltb4r1 inhibitor treatment also lowered serum insulin (Fig. 1f middle panel) and FFA (Fig. 1f right panel) levels. Comparable results were observed in Ltb4r1 inhibitor treated HFD/obese female ovariectomized (OVX) mice (Fig. S2). Together, these results indicate that the Ltb4r1 inhibitor confers a systemic insulin sensitive phenotype.

To quantitate this effect and to identify tissue specific responses, we performed hyperinsulinemic–euglycemic clamp studies, to assess insulin action in muscle, liver and adipose tissue *in vivo*. The Ltb4r1 inhibitor treated mice were substantially more insulin sensitive compared to HFD WT mice. This was manifested by an increased overall glucose infusion rate (GIR) (Fig. 1g left panel). In addition, the inhibitor treated mice exhibited enhanced insulin stimulated glucose disposal rate (IS–GDR, a measure of skeletal muscle insulin sensitivity) (Fig. 1g right panel), and an increased ability of insulin to suppress both hepatic glucose production (HGP) (Fig. 1h), as well as circulating FFA levels (Fig. 1i) (a measure of adipose tissue insulin sensitivity). Thus, Ltb4r1 inhibitor treatment led to greater *in vivo* insulin sensitivity in all 3 major insulin target tissues, muscle, liver, and fat. Furthermore, treatment of genetically obese *ob/ob* mice with the Ltb4r1 inhibitor (2 weeks) led to the expected increase in glucose tolerance (Fig. 1j left panel), no change in body weight (Fig. 1j middle panel) and decreased insulin levels (Fig. 1j right panel).

Effect of Ltb4r1 inhibition on *in vitro* and *in vivo* macrophage chemotaxis

It is known that LTB4 is a potent chemokine for macrophages, neutrophils, and T cells. As showed in Fig. 2a, LTB4 stimulated chemotaxis of IP–Macs in a dose dependent manner, and pre–treatment of the IP–Macs with the Ltb4r1 inhibitor blocked LTB4 induced chemotaxis (Fig. 2b). Adipocyte–conditioned medium (CM), contains a mixture of different chemokines, including Ccl2, Cxcl1, and LTB4. The Ltb4r1 inhibitor abolished CM–induced chemotaxis of both mouse IP–Macs and a human macrophage cell line U–937 without causing cell toxicity (Figs. 2c, 2d & S3), indicating that LTB4 is an important chemokine in adipose tissue CM. To determine if these *in vitro* chemotaxis results translated to the *in vivo* condition, we directly measured macrophage migration into adipose tissue using an *in vivo*

macrophage tracking technique[29]. With this approach, circulating monocytes were obtained from a WT donor mouse and labeled with fluorescent PKH26 dye *ex vivo*. The labeled monocytes were then injected into recipient HFD WT mice treated with the Ltb4r1 inhibitor or vehicle. As seen in Fig. 2e, there was a substantial decrease in labeled macrophage appearance in adipose tissue in the Ltb4r1 inhibitor treated mice. These data were more revealing when we examined the subpopulations of labeled macrophages between the groups. Thus, adipose tissue macrophages (ATMs) expressing Cd11c are M1–like and proinflammatory compared to M2–like Cd11c negative ATMs, which are non–inflammatory[30]. With this analysis, there is an even greater decrease in the number of recruited macrophages which express Cd11c, while, at the same time, there is an increase in the Cd11c⁻ macrophage population in the Ltb4r1 inhibitor treated mice. Indeed, the ratio of M1/M2 ATMs decreases from 9 to 2, indicative of improved adipose tissue homeostasis induced by Ltb4r1 inhibitor treatment. We also conducted *in vivo* monocyte tracking experiments with donor monocytes from either WT mice or Ltb4r1 KO mice injected into WT obese mice. We found that the ability of Ltb4r1 KO monocytes to migrate into adipose tissue was substantially impaired compared to WT cells (Fig. 2f), providing further support for the concept of decreased macrophage migration into tissues of Ltb4r1 inhibitor treated mice. Consistent with the IP–Mac chemotaxis and *in vivo* migration results, Fig. 2g shows reduced ATMs (F4/80$^+$, Cd11b$^+$, Cd11c$^{+/-}$, in red), Cd11c$^+$ ATMs (in purple), and adipose tissue neutrophils (ATNs) in Ltb4r1 inhibitor treated mice. Additionally, in *ob/ob* mice Ltb4r1 inhibition led to reduced Cd11c$^+$ ATMs and ATNs with higher Cd11c⁻ ATM content (Fig. 2h).

Inflammatory gene expression and cytokine levels in Ltb4r1 inhibitor treated mice

Consistent with the reduced ATM accumulation in HFD Ltb4r1 inhibitor treated mice, we also found decreased expression of a number of proinflammatory genes typically associated with the inflammatory/insulin resistant state in epididymal adipose tissue (Epi–WAT) (Fig. 3a). At the same time, an increase in anti–inflammatory gene expression, such as *Il–10, Mgl1, Clec7a*, *Mmr*, and *Il–4*, was observed in Epi–WAT (Fig. 3b). In addition to tissue inflammation, circulating cytokine levels are elevated in obesity, and as seen in figs. 3c–f, inflammatory cytokines levels were markedly reduced in HFD Ltb4r1 inhibitor treated compared to vehicle treated mice, as exemplified by Tnf-α, Il–6, Rantes, and Il–12p40. Epi–WAT mass and adipocyte size were not changed by Ltb4r1 inhibitor treatment (Fig. S5a & S5b).

LTB4 directly induces inflammation in macrophages

Decreased ATM content is one explanation for the reduced expression of proinflammatory markers in adipose tissue and blood (Figs. 2&3) in Ltb4r1 inhibitor treated mice. In addition, we considered the possibility that LTB4 could also directly activate intrinsic ATM pro–inflammatory pathways. To this end, we evaluated LTB4 inflammatory stimulation in isolated IP–Macs from WT and Ltb4r1 KO mice. We found that LTB4 stimulated phosphorylation of Ikkβ Jnk and B degradation (Fig. 4a).

To further demonstrate this concept, we measured the mRNA levels of different inflammatory and anti–inflammatory genes by qPCR. LTB4 generally stimulated

inflammatory cytokine gene expression, such as *Tnf-α, Il–6, Cxcl1*, and *Ccl2* (Fig. 4b), but did not affect the expression of anti–inflammatory genes (Fig. 4c). As evidence of a broader role for the LTB4/Ltb4r1 system in inflammatory responses, the Ltb4r1 inhibitor blocked LPS induced Jnk activation in IP–Macs from WT mice but was without effect on Ltb4r1 KO IP–Macs (Fig. 4d). As seen in Figs. 4e–j, LPS stimulated inflammatory gene expression was reduced in Ltb4r1 KO cells compared to WT, and the Ltb4r1 inhibitor decreased the LPS responses in WT IP–Macs to the same general level as seen in Ltb4r1 KO cells, while the compound had no effect in Ltb4r1 KO IP–Macs (Figs. 4e–j).

LTB4 directly induces cellular insulin resistance

Obesity–associated chronic tissue inflammation is a key mechanism for decreased insulin sensitivity, and the anti–inflammatory effects of the Ltb4r1 inhibitor or Ltb4r1 KO could explain the insulin sensitizing effects due to Ltb4r1 loss of function. However, we speculated that there was an additional, component, to the insulin sensitizing effects of Ltb4r1 inhibition. Thus, as seen in Fig. 1, LTB4 levels are elevated in all three major insulin target tissues, muscle, liver, and adipose from HFD/obese mice. Furthermore, we found that Ltb4r1 is well expressed in L6 myocytes and hepatocytes, but not in adipocytes (Fig. 5a). Most importantly, Fig. 5b demonstrates that LTB4 treatment of L6 myocytes directly inhibits insulin–stimulated glucose transport by ~50%. This LTB4 effect is accompanied by decreased insulin stimulated Akt phosphorylation (Fig. 5b right panel). Furthermore, LTB4 treatment inhibited Glut4 translocation in these cells (Fig. S5c), consistent with direct interference with insulin signaling in myocytes. Since Ltb4r1 signaling can couple with Gαi, we pre–treated cells with the Gαi inhibitor pertussis toxin (PT). As seen, PT blocked the effect of LTB4 to inhibit glucose transport (Fig.5b), indicating that Gαi mediates these LTB4 actions. In addition, PT treatment blocked the effects of LTB4 to inhibit insulin–stimulated Akt phosphorylation (Fig. S6a).

Irs1 serine phosphorylation can impair Irs1 downstream signaling, and it is well known that specific serine kinases can target Irs1. In our studies, we found that inhibition of Ikkβ or Erk by siRNA knockdown or small molecule inhibitors did not block the effects of LTB4 on Irs1 serine phosphorylation or subsequent steps in downstream insulin signaling (data not shown). On the other hand, our data indicate that Jnk activation is the likely intervening mechanism. Thus, Figure 5c shows that insulin stimulates Jnk phosphorylation, as has been well described, and that LTB4 treatment also stimulates Jnk activation. Interestingly, the combination of LTB4 and insulin stimulation produces additive effects on Jnk phosphorylation. Depletion of Jnk from L6 myocytes with siRNA is sufficient to completely block the effect of LTB4 treatment to inhibit insulin stimulated glucose transport (Fig. 5d left panel). Consistent with this, Jnk depletion blocks the effect of LTB4 to inhibit insulin stimulated Akt phosphorylation (Fig. 5d middle panel), and completely prevents the effect of LTB4 treatment to augment Irs1 serine phosphorylation (Fig. 5d right panel). Finally, we used a small molecule inhibitor of Jnk activity and found that pharmacologic Jnk inhibition had the same effects as siRNA depletion or KO on LTB4-induced cellular insulin resistance in L6 myocytes (Fig. S7). Taken together, these data are consistent with the view that LTB4 promotes cellular insulin resistance through a Gαi coupled mechanism which promotes Jnk

activation, leading to subsequent Irs1 serine phosphorylation with decreased downstream signaling through Akt to glucose transport in L6 cells.

In WT hepatocytes, we found that glucagon stimulates hepatic glucose output (HGO) and that this effect was completely inhibited by insulin (Fig. 5e, first three left hand sets of bars). LTB4 treatment of WT hepatocytes directly stimulated HGO, but was without effect in Ltb4r1 KO hepatocytes (Fig. 5e). This effect of LTB4 to stimulate HGO in WT cells was not inhibited by insulin, consistent with an LTB4 induced cellular insulin resistant state. Most importantly, LTB4 treatment blocked the effect of insulin to inhibit glucagon stimulated HGO in WT hepatocytes, but was without inhibitory effect in KO cells (Fig. 5e, right most bars). Thus, LTB4 stimulation can promote HGO by itself and can also attenuate insulin's normal inhibitory effects on this aspect of hepatic metabolism. Showing the specificity of this effect, LTB4 stimulated HGO can be completely blocked by Ltb4r1 inhibitor treatment (Fig. S8). The overall effect of glucagon to increase HGO was less in Ltb4r1 KO cells compared to WT (Fig. 5e), and the reason for this is unknown. In addition, insulin stimulated Akt phosphorylation in WT primary hepatocytes and this effect was completely inhibited by concomitant treatment with LTB4 (Fig.5f). In contrast, LTB4 had no effect to block Akt phosphorylation in Ltb4r1 KO hepatocytes (Fig. 5f). Similar to the results in L6 myocytes, LTB4 treatment led to hepatocyte Irs2 serine 307 phosphorylation (Fig. 5g). These effects of LTB4 to directly cause hepatocyte insulin resistance are mediated through Gαi signaling, as demonstrated by the fact that PT treatment prevented the effects of LTB4 to block insulin's inhibition of glucagon-stimulated HGO (Fig. 5h) and also blocked the effect of LTB4 to inhibit insulin stimulated Akt phosphorylation. (Fig. S6b). As with the L6 cells, siRNA-mediated depletion of Jnk blocked the effects of LTB4 to cause hepatocyte insulin resistance to HGO suppression (Fig. 5i).

In contrast to the effects of the LTB4/Ltb4r1 system on insulin action in myocytes and hepatocytes, LTB4 did not inhibit insulin-stimulated glucose transport in 3T3-L1 adipocytes (data not shown). This is fully consistent with the results in Fig. 5a, showing that Ltb4r1 is not expressed in these cells.

In vivo studies on clodronate and Ltb4r1 inhibitor treatment

To try and dissect the contribution of these different effects of LTB4 insulin sensitivity *in vivo*, we deleted macrophages in control and Ltb4r1 inhibitor treated mice by clodronate injection. Consistent with previous finding, the clodronate injection greatly improves glucose tolerance in HFD mice (Fig. 5j left panel), and this is accompanied by decreased circulating insulin levels (Fig. 5j right panel), showing that deletion of macrophages alone is sufficient to greatly improve insulin resistance. However, clodronate plus Ltb4r1 inhibitor treated mice were ~40% more glucose tolerant than the veh/clodronate treated group with a further ~60% reduction in plasma insulin levels (Fig. 5j), and these values are even lower than the glucose and insulin levels in chow-fed mice (Fig. S1). These results indicates that the *in vivo* insulin sensitizing effects of the Ltb4r1 inhibitor are mediated through a combination of an anti-inflammatory effect in immune cells and direct insulin sensitizing effects on insulin target cells.

Hepatic lipid profile

It's known that HFD/obesity leads to marked hepatosteatosis[31,32]. Interestingly, after 2 weeks of Ltb4r1 inhibitor treatment, hepatic fat accumulation was largely absent in both HFD and *ob/ob* mice (Fig. 6a), and this was accompanied by reduced expression of the lipogenic genes, *Lxrα, Srebp1c, Ldlr* (Fig. 6b).

In primary hepatocytes, we found that LTB4 treatment directly increased *de novo* synthesis of hepatic DAGs and ceramides (Figs. 6c&d). Since ceramide and DAGs have been reported to inhibit insulin action, this provides a possible further mechanism for hepatic insulin resistance[33–37].

Discussion

Here we show that inhibition of Ltb4r1 results in an anti–inflammatory phenotype with protection from systemic insulin resistance in the setting of both HFD-induced and genetic obesity. This robust phenotype in the Ltb4r1 inhibitor treated mice was manifested by decreased macrophage accumulation in adipose tissue, decreased expression of inflammatory pathway genes, reduced blood cytokine levels, and decreased hepatic steatosis. In addition, we observed improved glucose tolerance, as well as systemic insulin sensitivity as measured by the hyperinsulinemic euglycemic clamp method, in Ltb4r1 inhibitor treated animals. Importantly, treatment with LTB4 stimulated inflammatory pathways in macrophages and directly caused cellular insulin resistance in hepatocytes and myocytes. This improvement in inflammatory status and insulin sensitivity reinforces the connection between chronic tissue inflammation and insulin resistance. Given that macrophages, other immune cells and insulin target cells can all produce LTB4, the effect of LTB4 to promote inflammation, along with its direct effects to cause cellular insulin resistance in hepatocytes and myocytes, adds a new layer of understanding to the inflammation/insulin resistance syndrome.

There is a significant literature showing that LTB4 is a potent chemotatic factor operating through Ltb4r1 and Ltb4r2[38,39]. Ltb4r1 is more specifically distributed on macrophages neutrophils[40] and lymphocytes[41], and both the KO mice and the selective inhibitor represent specific loss of function studies directed only at Ltb4r1. These studies suggest that obesity–associated production of LTB4 by primary tissue cells such as adipocytes, hepatocytes, myocytes, endothelial cells, or other resident tissue cell types could be an early trigger for the chronic tissue inflammatory state in obesity. LTB4 acts as a powerful chemokine, working through Ltb4r1 on immune cell types, to cause chemotaxis and migration into tissues. Strong support for this notion comes from the *in vitro* chemotaxis and *in vivo* monocyte tracking experiments in HFD and *ob/ob* mice. Thus, Ltb4r1 inhibition impairs chemotaxis and tracking of monocytes and other immune cells into adipose tissue, inhibiting the ultimate inflammation/insulin resistance syndrome. This is consistent with recent studies in Ltb4r1 KO mice, showing an anti-inflammatory phenotype, along with improved glucose tolerance and insulin sensitivity.

In addition to its inflammatory effects related to immune cell recruitment, the LTB4/Ltb4r1 system also exerts direct proinflammatory actions in macrophages. Thus, we show that

treatment of WT IP–Macs with LTB4 leads to stimulation of the Ikkβ/NfκB and Jnk/Ap1 pathways and that this effect is absent in Ltb4r1 KO IP-Macs. Although we did not study direct effect of LTB4 on lymphocytes or neutrophils, previous work has shown proinflammatory effects of LTB4 in these cell types[40,41]. In this context, it is important to note that LTB4 can also be produced by recruited immune cells, setting up a positive reinforcing vicious cycle. Thus, tissue cells, such as adipocytes, produce LTB4, which recruits and activates ATMs; these immune cells then elaborate more LTB4, further propagating the chronic tissue inflammatory response. This could be a new mechanism for inflammation-induced insulin resistance, since LTB4 is downstream of all the major proinflammatory pathways and is elevated in the three key insulin target tissues.

One of the novel findings in this study is that LTB4 can directly cause insulin resistance in muscle and liver cells. This component of insulin resistance is independent of effects of LTB4/Ltb4r1 to promote tissue inflammation. Although production of LTB4 is part of an inflammatory response, in a certain sense, this can be looked at as a more direct mechanism of insulin resistance. As demonstrated, this mechanism operates in both myocytes and hepatocytes, but not adipocytes, as the latter do not express Ltb4r1. Since the euglycemic glucose clamp studies demonstrate systemic insulin resistance in all three major insulin target tissues, we conclude that the adipose tissue insulin sensitivity conferred by Ltb4r1 inhibitor treatment is mainly due to attenuation of the adipose tissue inflammatory response. With respect to mechanisms of the direct effects of LTB4 to induce insulin resistance, our studies indicate that LTB4 works specifically through Ltb4r1 in hepatocytes and myocytes to interfere with proximal steps of insulin signaling. It is known that Irs1and Irs2 serine phosphorylation can inhibit Irs1 and Irs2 activity, blunting downstream signaling events[42]. Indeed, we show that LTB4 treatment enhances Irs2 serine phosphorylation in hepatocytes. All of these LTB4 effects are coupled to Gαi signaling, since they are inhibited by concomitant treatment with the Gαi inhibitor PT. Furthermore, we found that LTB4 stimulated Jnk kinase activity, mediating the inhibitory Irs1/2 serine phosphorylation events. Both genetic and pharmacologic Jnk loss of function inhibits all the effects of LTB4 to induce cellular insulin resistance in isolated hepatocytes and L6 myocytes. Taken together, these results provide a reasonable Gαi/Jnk dependent molecular mechanism for LTB4 induced cellular insulin resistance.

Our data indicate that these direct effects of LTB4 to cause decreased myocyte and hepatocyte insulin sensitivity are operative *in vivo*. Thus, macrophage depletion in clodronate treated mice caused a marked improvement in glucose tolerance and hyperinsulinemia, while clodronate plus Ltb4r1 inhibitor treatment led to a 40-60% further reduction in glucose or insulin levels, respectively. This is consistent with the view that blockade of Ltb4r1 *in vivo* can improve insulin signaling by both attenuating obesity-induced inflammation and interfering with the direct effects of LTB4 to cause cellular insulin resistance.

The effect of LTB4 to directly cause decreased insulin sensitivity may have important potential translational implications. Thus, while there are likely multiple mechanisms for insulin resistance[46], it has been known for several years that chronic tissue inflammation is a key cause of decreased *in vivo* insulin sensitivity. However, therapeutic efforts to ameliorate

this inflammation induce insulin resistance have had limited success[47]. While some studies have shown glucose lowering effects[48,49] of specific TNF-α or IL-1β inhibitors, these agents have had small to no effects at improving insulin sensitivity in clinical studies[47-51], Even the more general anti- inflammatory agent salsalate has had only modest effects[47,52-54]. IL-1β inhibition does lead to glucose lowering effects[55,56], but these have been ascribed to enhanced β cell functions, not improved insulin sensitivity[48,55,56]. Based on the current studies, one can raise the possibility that these therapeutic modalities are not fully directed at the mechanisms for insulin resistance and that attempts to inhibit the LTB4/Ltb4r1 system might be efficacious.

It is of interest that after Ltb4r1 inhibitor treatment, a marked resolution of hepatic steatosis was observed in both HFD and *ob/ob* mice. Interestingly, *in vitro* treatment of primary hepatocytes with LTB4 stimulated the production of DAGs as well as ceramides. This is potentially important, since both of these lipid metabolites have been suggested as causative factors in hepatic insulin resistance[33,36].

In summary, these results show that LTB4 is overexpressed in insulin target tissues in obesity and that the LTB4/Ltb4r1 system is a major driver for the inflammation/insulin resistance syndrome. Thus, LTB4 is a potent chemokine promoting migration of monocytes into adipose tissue and directly stimulates macrophage Ltb4r1 to activate intracellular proinflammatory pathways. Our studies also reveal a novel additional mechanism for LTB4-induced insulin resistance. Thus, *in vitro*, LTB4 directly caused decreased insulin sensitivity in hepatocytes and myocytes. This cytokine-independent mechanism of insulin resistance provides a new mechanism connecting inflammation and decreased insulin sensitivity. As such, it is possible that inhibition of LTB4 action could be a useful future therapeutic goal in the treatment of insulin resistance diseases.

Online methods

Animal care and use

Animals were housed in an animal facility on a 12 h/12 h light/dark cycle with free access to food and water. All animal procedures were in accordance with University of California San Diego research guidelines for the care and use of laboratory animals.

Ltb4r1 inhibitor

The Ltb4r1 inhibitor, CP-105696, was provided by Pfizer and this compound is highly specific for Ltb4r1 compared to Ltb4r2[57], The structure is provided in references 27 and 28. 8 week old mice (C57BL6/J) were fed 60% HFD for 14 weeks and the Ltb4r1 inhibitor (50 mg kg^{-1}) was orally gavaged daily for 2 weeks beginning at 12 weeks of HFD (n=10 in each group). *Ob/ob* mice (6 weeks old, n=10 in each group) were gavaged at the dose of 50 mg kg^{-1} daily for 2 weeks.

Clodronate treatment

8 week old mice (C57BL6/J) were fed 60% HFD for 14 weeks and the Ltb4r1 inhibitor (50 mg kg^{-1}) was orally gavaged daily for 3 weeks beginning at 12 weeks of HFD (n=12 in each

group). After 2 weeks of treatment, mice in vehicle and inhibitor groups were given clodronate (intraperitoneal; 100 mg kg^{-1}) or PBS, followed by second and third injections every 3 days. After 10 days from the first injection, glucose tolerance tests were performed. As previously described, clodronate treatment deleted most of the macrophages in WAT[58].

ITTs, GTTs, and hyperinsulinemic euglycemic clamp study

For glucose tolerance tests (GTTs), animals were IP injected with dextrose (1 g kg^{-1}, Hospira, Inc) after 6 hours of fasting, and blood was drawn to measure blood glucose at 0, 15, 30, 60, and 120 minutes after dextrose injection. For insulin tolerance test (ITTs), 0.5 units kg^{-1} of insulin (Novolin R, Novo-Nordisk) was IP injected after 6 hours of fasting, and blood was drawn at 0, 15, 30, 60 and 90 minutes after insulin injection. Glucose clamps were performed as previously described[59-61].

SVCs isolation, and FACS analysis

Stromal vascular cells (SVCs) isolation and FACS analyses were performed as previously described[61,62]. Briefly, epididymal fat pads were weighed, rinsed three times in PBS, and then minced in 1% BSA PBS. Tissue suspensions were digested with collagenase (1 mg ml^{-1}, Sigma-Aldrich) for 30 minutes. After centrifugation at 500 g for 5 min, the pellet containing SVCs was incubated with red blood cell (RBC) lysis buffer (eBioscience) for 5 min followed by another centrifugation (300 g, 5 min) and resuspension in 1% BSA PBS. SVCs were incubated with Fc Block (BD Biosciences) for 20 min at 4 °C before staining with fluorescently labeled primary antibodies or control IgGs for 30 min at 4 °C. F4/80-APC FACS antibody was purchased from AbD Serotec (Raleigh, NC); FITC-Cd11b, PE-Cd11c and APC- Cy7-Ly6G antibodies were from BD Biosciences.

Phenotypic evaluation of mice

Male mice ($n = 20$) were fed with 60% high fat diet (HFD) for 14 weeks, and received vehicle or Ltb4r1 inhibitor for 2 weeks at the dose of 50 mg kg^{-1} once a day by oral gavage (n=10 in each group) starting at 12 weeks HFD. Plasma insulin was measured with ELISA kits from ALPCO. Plasma FFA levels were measured enzymatically using a kit from WAKO Chemicals. Serum Il-6, Rantes, Tnf-α and Il-12p40 levels were measured using a multiplex Luminex assay (Millipore/Linco research).

Immunohistochemistry

Liver was fixed and embedded in paraffin and sectioned for HE staining.

In vitro chemotaxis assay

In vitro chemotaxis assay was performed as previously described[63]. Briefly, mouse thioglycollate-elicited peritoneal macrophages were isolated from WT mice. For the migration *per se*, 100,000 intraperitoneal macrophages (IPMacs) were placed in the upper chamber of an 8 μm polycarbonate filter (24-transwell format; Corning, Lowell, MA) with or without Ltb4r1 inhibitor for 30 min; primary adipocyte conditioned medium or DMEM with LTB4 (Cayman Chemical) was placed in the lower chamber. After 3 hr of migration, cells were fixed in formalin and stained with 4′, 6-diamidino-2-phenylindole and counted.

In vivo monocytee tracking

Leukocyte pools from C57BL/6 WT or Ltb4r1 KO mice, bled by retro orbital sinus, were subjected to RBC lysis buffer and monocyte subsets were enriched with EasySep® mouse monocyte enrichment kit (STEMCELL tech, Vancouver, BC) following the manufacture's instructions. Isolated monocytes (2×10^6 to 5×10^6) were washed once in serum-free medium (RPMI-1640) and suspended in 2 ml of Diluent solution C (included in the PKH26 labeling kit). Two ml of PKH26 (Sigma Chemical Co. St Louis, MO) at 2×10^{-3} M in Diluent C was added and mixed, and the cells were incubated for 10 min at room temperature in the dark. The staining reaction was stopped by addition of an equal volume (2 ml) of medium supplemented with 10% FBS. The mixture was centrifuged and the cells were washed once and resuspended in serum containing medium. Subsequent to labeling with PKH26, the monocytes were counted and ~0.5×10^6 viable cells were suspended in 0.2 ml PBS and *i.v.* injected into retroorbitally in each group of mice. Five days after injection, SVCs isolated from visceral fat tissue and analyzed by FACS.

Cell culture and reagents

Mouse thioglycollate-elicited peritoneal macrophages and bone marrow derived macrophages were obtained and cultured as described previously[64]. For gene expression studies, cells were cultured in medium containing DMEM with low glucose overnight, treated with or without Ltb4r1 inhibitor (10 μM) for 1 hour, and then stimulated with LPS (100 ng ml^{-1}), or LTB4 (100 nM) for 6hr. For inflammatory signaling experiments, cells were pretreated with either vehicle (DMSO) or 100 nM of Ltb4r1 inhibitor for 1 hour, then treated with LPS (100 ng ml^{-1}) or LTB4 (100 nM) for 45 min. LPS was purchased from Sigma, LTB4 was purchased from Cayman Chemical.

Glucose uptake in L6 muscle cells

L6 rat skeletal myoblasts were obtained as gifts from Amira Klip's laboratory at The Hospital for Sick Children, Toronto, ON, Canada. Myoblasts were–MEM with 10% FBS and antibiotics. After cultures reached 80-90% confluency, medium was switched to 2% FBS to allow differentiation and myotube formation. After 8-10 days, cultures were used for experiments. On the day of experiment, cultures were serum-starved for 6 hours in α-MEM containing 0.2% fatty acid free BSA and then switched to hepes–phosphate salt buffer containing 10 mM Hepes, 4 mM KCl, 125 mM NaCl, 0.83 mM KH2PO4, 1.27 mM Na2HPO4, 1 mM MgSO4, 1mM CaCl2 and 0.2% fatty acid free BSA, pH 7.4. Cells were treated with vehicle (0.1% ethanol) or 100 nM LTB4 for 45 minutes and 100 nM insulin for 30 minutes. In one set of cultures, treatment started with LTB4 and, 15 minutes later, insulin was added and incubated for an additional 30 minutes. All cultures were exposed to [3H]-2-deoxy- glucose (100 nM, 0.4 μCi ml^{-1}) for the last 10 minutes of incubation. Incubations were terminated by aspiration of radiolabeled culture buffer followed by washing twice with cold PBS. Cells were dissolved in 1 N NaOH and an aliquot was used for protein estimation and the rest of the extracts were transferred to scintillation vials, neutralized with 1 N HCl, mixed with scintillation fluid and counted for radioactivity.

Glucose output assay in mouse hepatocytes

Mice were infused through the inferior vena cava with a calcium free hepes-phosphate buffer (pH 7.4) for 10 minutes followed by a collagenase solution (Liberase TM from Roche) for 10 minutes. The digested livers were excised, hepatocytes were collected and washed five times in buffer by centrifuging at $70 \times g$ for 5 minutes. Cells were further purified by centrifugation ($2400 \times g$ for 10 minutes) over percoll density gradient (1.06 g/ml). Primary mouse hepatocytes were allowed to attach for 6 hours on collagen-coated plates in Medium E fortified with non-essential amino acids, glutamax, antibiotics, 10% FBS and dexamethasone (10 nM) and cultured overnight in the same medium without serum. Cultures were then washed in hepes phosphate-salt-bicarbonate (HPSB) buffer (10 mM Hepes, 4 mM KCl, 125 mM NaCl, 0.85 mM KH_2PO_4, 1.25 mM Na_2HPO_4, 1 mM $MgCl_2$, 1 mM $CaCl_2$ and 15 mM $NaHCO_3$) containing 0.2% fatty acid free BSA, and incubated in the same buffer containing LTB4, insulin or glucagon and substrates in a 5% CO_2 incubator. 14C-Pyruvate (2 mM, 0.5 µCi Pyruvate/incubation) was used as substrate. Incubations were carried out in 0.5 ml buffer in 24–well plates containing 0.25 million cells/well. Cells were pre-incubated (in absence of substrate) for 1 hour with vehicle (0.1% ethanol), LTB4 (30 nM for 1 hour), insulin (10 nM for 30 minutes) or glucagon (10 ng ml^{-1} for 30 minutes), LTB4 for the first 30 minutes and then with insulin for an additional 30 minutes, LTB4 for first 30 minutes and then with insulin and glucagon for additional 30 minutes. These pre-incubations were followed by incubation with the substrate for 3 hours. At the end of incubation, buffers were transferred to 1.7 ml microfuge tubes and added 0.25 ml 5% $ZnSO_4$ and 0.25 ml 0.3 N $Ba(OH)_2$ suspensions to each tube followed by 0.5 ml water. After centrifugation, supernatants were transferred to a fresh set of tubes and assayed for radiolabeled glucose released into the media by separating radiolabeled glucose by mixed bed ion-exchange resins, AG-501x8 resins (BioRad). 200 mg resins were added to each tube, vortexed intermittently for 15 min, centrifuged and the supernatants were transferred to scintillation vials for counting radioactivity. Cells on the plates were dissolved in 1N NaOH for protein estimation.

Jnk inhibitor and Jnk siRNA

The Jnk inhibitor was purchased from EMD Sciences. L6 myocytes were treated with the Jnk inhibitor (100 nM) for 0.5 hour before the LTB4 treatment. Jnk siRNA and Ctrl siRNA were purchased from cell signaling. The X-tremeGENE siRNA transfection reagent (Roche applied Science) was used to transfect Jnk or Ctrl siRNA into L6 myocytes or primary hepatocytes. After 18 hours transfection, glucose uptake assays or glucose production assays were performed in L6 myocytes and hepatocytes, respectively.

PT treatment

PT was purchased from Calbiochem and treated to L6 myocytes or hepatocytes for 12 hours at the dose of 100 ng ml^{-1} before the glucose uptake or glucose production assays.

Lipogenesis from 14C-palmitate: DAG and Ceramide production

Hepatocytes in HPSB buffer were incubated with 1-14C-Palmitate (0.2 mM, 0.5 µCi ml^{-1}) in the presence of vehicle (0.1% ethanol), LTB4 (30 nM) and insulin (10 nM). Hepatocytes

were incubated with the agonists for 30 minutes and 2 hours. Incubations were terminated by adding 0.25 ml methanol containing 1N HCl to the culture wells. Solvents were transferred to fresh microfuge tubes and the extraction was repeated. Chloroform (0.25 ml) and water (0.5 ml) were added to the combined extracts. The mixtures were vortexed and centrifuged to separate two layers. The lower organic layers were collected, evaporated and aliquots were counted to determine incorporation into total lipids. DAG and ceramides were separated from other lipids by thin layer chromatography (TLC) by following a published method[65] and their identities were confirmed by the formation of phosphatidic acid and ceramide-1-phosphate by the reactions with DAG kinase and ceramide kinase respectively as per the published methods[66,67] Lipid spots on the TLC plates were detected by iodine vapor. Spots were scraped off and radioactivity in the DAG and ceramide spots was determined.

Tissue LTB4 measurement

C57BL/6J mice were put on HFD for 14 weeks from 8 weeks of age, then tissues (liver, quadriceps muscle and Epi-WAT) were collected from HFD and age matched NC mice. n=6 in each group. LTB4 measurement was performed as previously described[68].

Data Analysis

Densitometric quantification and normalization were performed using the ImageJ 1.42q software. The values presented are expressed as the means ± s.e.m. The statistical significance of the differences between various treatments was determined by one-way analysis of variance with the Bonferroni correction using GraphPad Prism 6.0 (San Diego, CA). $P < 0.05$ was considered significant. No statistical method was used to predetermine sample size. The experiments were not randomized. The investigators were not blinded to allocation during experiments and outcome assessment.

Supplementary Material

Refer to Web version on PubMed Central for supplementary material.

Acknowledgements

References

1. Haffner S, Taegtmeyer H. Epidemic obesity and the metabolic syndrome. Circulation. 2003; 108:1541–1545. [PubMed: 14517149]

2. Olefsky JM, Glass CK. Macrophages, inflammation, and insulin resistance. Annu Rev Physiol. 2010; 72:219–246. [PubMed: 20148674]

3. Reaven GM. The insulin resistance syndrome: definition and dietary approaches to treatment. Annu Rev Nutr. 2005; 25:391–406. [PubMed: 16011472]

4. Olefsky JM, et al. Cellular mechanisms of insulin resistance in non–insulin–dependent (type II) diabetes. The American journal of medicine. 1988; 85:86–105. [PubMed: 3057897]

5. Hotamisligil GS, Shargill NS, Spiegelman BM. Adipose expression of tumor necrosis factor-alpha: direct role in obesity-linked insulin resistance. Science. 1993; 259:87–91. [PubMed: 7678183]

6. Shoelson SE, Lee J, Yuan M. Inflammation and the IKK beta/I kappa B/NF-kappa B axis in obesity- and diet-induced insulin resistance. Int J Obes Relat Metab Disord. 2003; 27(Suppl 3):S49–52. [PubMed: 14704745]

7. Mathis D. Immunological goings-on in visceral adipose tissue. Cell metabolism. 2013; 17:851–859. [PubMed: 23747244]

8. Weisberg SP, et al. Obesity is associated with macrophage accumulation in adipose tissue. J Clin Invest. 2003; 112:1796–1808. [PubMed: 14679176]

9. Xu H, et al. Chronic inflammation in fat plays a crucial role in the development of obesity-related insulin resistance. J Clin Invest. 2003; 112:1821–1830. [PubMed: 14679177]

10. Lanthier N, et al. Kupffer cell activation is a causal factor for hepatic insulin resistance. Am J Physiol Gastrointest Liver Physiol. 2009; 298:G107–116. [PubMed: 19875703]

11. Pillon NJ, Bilan PJ, Fink LN, Klip A. Cross-talk between skeletal muscle and immune cells: muscle-derived mediators and metabolic implications. American journal of physiology. Endocrinology and metabolism. 2013; 304:E453–465. [PubMed: 23277185]

12. Chawla A, Nguyen KD, Goh YP. Macrophage-mediated inflammation in metabolic disease. Nature reviews. Immunology. 2011; 11:738–749.

13. Kintscher U, et al. T-lymphocyte infiltration in visceral adipose tissue: a primary event in adipose tissue inflammation and the development of obesity-mediated insulin resistance. Arterioscler Thromb Vasc Biol. 2008; 28:1304–1310. [PubMed: 18420999]

14. Wu D, et al. Eosinophils sustain adipose alternatively activated macrophages associated with glucose homeostasis. Science. 2011; 332:243–247. [PubMed: 21436399]

15. Yang H, et al. Obesity increases the production of proinflammatory mediators from adipose tissue T cells and compromises TCR repertoire diversity: implications for systemic inflammation and insulin resistance. J Immunol. 2010; 185:1836–1845. [PubMed: 20581149]

16. Samuelsson B, Dahlen SE, Lindgren JA, Rouzer CA, Serhan CN. Leukotrienes and lipoxins: structures, biosynthesis, and biological effects. Science. 1987; 237:1171–1176. [PubMed: 2820055]

17. Kim N, Luster AD. Regulation of immune cells by eicosanoid receptors. The Scientific World Journal. 2007; 7:1307–1328. [PubMed: 17767352]

18. Tager AM, Luster AD. Ltb4r1 and Ltb4r2: the leukotriene B(4) receptors. Prostaglandins, leukotrienes, and essential fatty acids. 2003; 69:123–134.

19. Toda A, Yokomizo T, Shimizu T. Leukotriene B4 receptors. Prostaglandins & other lipid mediators. 2002; 68-69:575–585. [PubMed: 12432944]

20. Chou RC, et al. Lipid-cytokine-chemokine cascade drives neutrophil recruitment in a murine model of inflammatory arthritis. Immunity. 2010; 33:266–278. [PubMed: 20727790]

21. Haribabu B, et al. Targeted disruption of the leukotriene B(4) receptor in mice reveals its role in inflammation and platelet-activating factor-induced anaphylaxis. The Journal of experimental medicine. 2000; 192:433–438. [PubMed: 10934231]

22. Subbarao K, et al. Role of leukotriene B4 receptors in the development of atherosclerosis: potential mechanisms. Arteriosclerosis, thrombosis, and vascular biology. 2004; 24:369–375.

23. Spite M, et al. Deficiency of the leukotriene B4 receptor, BLT-1, protects against systemic insulin resistance in diet-induced obesity. Journal of immunology. 2011; 187:1942–1949.

24. Yokomizo T, Kato K, Hagiya H, Izumi T, Shimizu T. Hydroxyeicosanoids bind to and activate the low affinity leukotriene B4 receptor, Ltb4r2. The Journal of biological chemistry. 2001; 276:12454–12459. [PubMed: 11278893]

25. Liston TE, et al. Pharmacokinetics and pharmacodynamics of the leukotriene B4 receptor antagonist CP-105,696 in man following single oral administration. British journal of clinical pharmacology. 1998; 45:115–121. [PubMed: 9491823]

26. Aiello RJ, et al. Leukotriene B4 receptor antagonism reduces monocytic foam cells in mice. Arteriosclerosis, thrombosis, and vascular biology. 2002; 22:443–449.

27. Showell HJ, Breslow R, Conklyn MJ, Hingorani GP, Koch K. Characterization of the pharmacological profile of the potent LTB4 antagonist CP-105,696 on murine LTB4 receptors in vitro. British journal of pharmacology. 1996; 117:1127–1132. [PubMed: 8882606]

28. Hicks A, Monkarsh SP, Hoffman AF, Goodnow R Jr. Leukotriene B4 receptor antagonists as therapeutics for inflammatory disease: preclinical and clinical developments. Expert opinion on investigational drugs. 2007; 16:1909–1920. [PubMed: 18042000]

29. Oh DY, Morinaga H, Talukdar S, Bae EJ, Olefsky JM. Increased macrophage migration into adipose tissue in obese mice. Diabetes. 2012; 61:346–354. [PubMed: 22190646]

30. Lumeng CN, Bodzin JL, Saltiel AR. Obesity induces a phenotypic switch in adipose tissue macrophage polarization. J Clin Invest. 2007; 117:175–184. [PubMed: 17200717]

31. Birkenfeld AL, Shulman GI. Non alcoholic fatty liver disease, hepatic insulin resistance and type 2 diabetes. Hepatology. 2013

32. Samuel VT, et al. Mechanism of hepatic insulin resistance in non-alcoholic fatty liver disease. The Journal of biological chemistry. 2004; 279:32345–32353. [PubMed: 15166226]

33. Kumashiro N, et al. Cellular mechanism of insulin resistance in nonalcoholic fatty liver disease. Proc Natl Acad Sci U S A. 2011; 108:16381–16385. [PubMed: 21930939]

34. Jornayvaz FR, Shulman GI. Diacylglycerol activation of protein kinase Cepsilon and hepatic insulin resistance. Cell metabolism. 2012; 15:574–584. [PubMed: 22560210]

35. Holland WL, et al. Lipid-induced insulin resistance mediated by the proinflammatory receptor TLR4 requires saturated fatty acid-induced ceramide biosynthesis in mice. J Clin Invest. 2011; 121:1858–1870. [PubMed: 21490391]

36. Pagadala M, Kasumov T, McCullough AJ, Zein NN, Kirwan JP. Role of ceramides in nonalcoholic fatty liver disease. Trends in endocrinology and metabolism: TEM. 2012; 23:365–371. [PubMed: 22609053]

37. Chavez JA, Summers SA. A ceramide-centric view of insulin resistance. Cell metabolism. 2012; 15:585–594. [PubMed: 22560211]

38. Islam SA, et al. The leukotriene B4 lipid chemoattractant receptor Ltb4r1 defines antigen-primed T cells in humans. Blood. 2006; 107:444–453. [PubMed: 16179368]

39. Weller CL, et al. Leukotriene B4, an activation product of mast cells, is a chemoattractant for their progenitors. The Journal of experimental medicine. 2005; 201:1961–1971. [PubMed: 15955837]

40. Afonso PV, et al. LTB4 is a signal-relay molecule during neutrophil chemotaxis. Developmental cell. 2012; 22:1079–1091. [PubMed: 22542839]

41. Yamaoka KA, Claesson HE, Rosen A. Leukotriene B4 enhances activation, proliferation, and differentiation of human B lymphocytes. Journal of immunology. 1989; 143:1996–2000.

42. Boura-Halfon S, Zick Y. Phosphorylation of IRS proteins, insulin action, and insulin resistance. American journal of physiology. Endocrinology and metabolism. 2009; 296:E581–591. [PubMed: 18728222]

43. Lee YH, Giraud J, Davis RJ, White MF. c-Jun N-terminal kinase (JNK) mediates feedback inhibition of the insulin signaling cascade. The Journal of biological chemistry. 2003; 278:2896–2902. [PubMed: 12417588]

44. Gao Z, et al. Serine phosphorylation of insulin receptor substrate 1 by inhibitor kappa B kinase complex. The Journal of biological chemistry. 2002; 277:48115–48121. [PubMed: 12351658]

45. Aguirre V, Uchida T, Yenush L, Davis R, White MF. The c-Jun NH(2)-terminal kinase promotes insulin resistance during association with insulin receptor substrate-1 and phosphorylation of Ser(307). The Journal of biological chemistry. 2000; 275:9047–9054. [PubMed: 10722755]

46. Garvey WT, Olefsky JM, Marshall S. Insulin induces progressive insulin resistance in cultured rat adipocytes. Sequential effects at receptor and multiple postreceptor sites. Diabetes. 1986; 35:258–267. [PubMed: 3512337]

47. Donath MY, Dalmas E, Sauter NS, Boni-Schnetzler M. Inflammation in obesity and diabetes: islet dysfunction and therapeutic opportunity. Cell metabolism. 2013; 17:860–872. [PubMed: 23747245]

48. Larsen CM, et al. Interleukin-1-receptor antagonist in type 2 diabetes mellitus. The New England journal of medicine. 2007; 356:1517–1526. [PubMed: 17429083]

49. Stanley TL, et al. TNF-alpha antagonism with etanercept decreases glucose and increases the proportion of high molecular weight adiponectin in obese subjects with features of the metabolic syndrome. The Journal of clinical endocrinology and metabolism. 2011; 96:E146–150. [PubMed: 21047923]

50. Kiortsis DN, Mavridis AK, Vasakos S, Nikas SN, Drosos AA. Effects of infliximab treatment on insulin resistance in patients with rheumatoid arthritis and ankylosing spondylitis. Annals of the rheumatic diseases. 2005; 64:765–766. [PubMed: 15458960]

51. Ofei F, Hurel S, Newkirk J, Sopwith M, Taylor R. Effects of an engineered human anti-TNF-alpha antibody (CDP571) on insulin sensitivity and glycemic control in patients with NIDDM. Diabetes. 1996; 45:881–885. [PubMed: 8666137]

52. Goldfine AB, et al. Targeting Inflammation Using Salsalate in Patients With Type 2 Diabetes (TINSAL): Effects on flow-mediated dilation. Diabetes care. 2013

53. Goldfine AB, et al. A randomised trial of salsalate for insulin resistance and cardiovascular risk factors in persons with abnormal glucose tolerance. Diabetologia. 2013; 56:714–723. [PubMed: 23370525]

54. Goldfine AB, et al. Salicylate (salsalate) in patients with type 2 diabetes: a randomized trial. Annals of internal medicine. 2013; 159:1–12. [PubMed: 23817699]

55. Cavelti-Weder C, et al. Effects of gevokizumab on glycemia and inflammatory markers in type 2 diabetes. Diabetes care. 2012; 35:1654–1662. [PubMed: 22699287]

56. Sloan-Lancaster J, et al. Double-blind, randomized study evaluating the glycemic and anti-inflammatory effects of subcutaneous LY2189102, a neutralizing IL-1beta antibody, in patients with type 2 diabetes. Diabetes care. 2013; 36:2239–2246. [PubMed: 23514733]

References

57. Yokomizo T, Kato K, Hagiya H, Izumi T, Shimizu T. Hydroxyeicosanoids bind to and activate the low affinity leukotriene B4 receptor, LTB4R2. The Journal of biological chemistry. 2001; 276:12454–12459. [PubMed: 11278893]

58. Lee YS, et al. Inflammation is necessary for long-term but not short-term high-fat diet-induced insulin resistance. Diabetes. 2011; 60:2474–2483. [PubMed: 21911747]

59. He W, et al. Adipose-specific peroxisome proliferator-activated receptor gamma knockout causes insulin resistance in fat and liver but not in muscle. Proc Natl Acad Sci U S A. 2003; 100:15712–15717. [PubMed: 14660788]

60. Lu M, et al. Inducible nitric oxide synthase deficiency in myeloid cells does not prevent diet-induced insulin resistance. Mol Endocrinol. 2010; 24:1413–1422. [PubMed: 20444886]

61. Li P, et al. Functional heterogeneity of CD11c-positive adipose tissue macrophages in diet-induced obese mice. The Journal of biological chemistry. 2010; 285:15333–15345. [PubMed: 20308074]

62. Lee YS, et al. Increased adipocyte O2 consumption triggers HIF-1alpha, causing inflammation and insulin resistance in obesity. Cell. 2014; 157:1339–1352. [PubMed: 24906151]

63. Oh DY, et al. GPR120 is an omega-3 fatty acid receptor mediating potent anti- inflammatory and insulin-sensitizing effects. Cell. 2010; 142:687–698. [PubMed: 20813258]

64. Li P, et al. NCoR repression of LXRs restricts macrophage biosynthesis of insulin- sensitizing omega 3 fatty acids. Cell. 2013; 155:200–214. [PubMed: 24074869]

65. Bodennec J, Brichon G, Koul O, El Babili M, Zwingelstein G. A two- dimensional thin-layer chromatography procedure for simultaneous separation of ceramide and diacylglycerol species. Journal of lipid research. 1997; 38:1702–1706. [PubMed: 9300792]

66. Bielawska A, Perry DK, Hannun YA. Determination of ceramides and diglycerides by the diglyceride kinase assay. Analytical biochemistry. 2001; 298:141–150. [PubMed: 11757501]

67. Bektas M, Jolly PS, Milstien S, Spiegel S. A specific ceramide kinase assay to measure cellular levels of ceramide. Analytical biochemistry. 2003; 320:259–265. [PubMed: 12927832]

68. Quehenberger O, et al. Lipidomics reveals a remarkable diversity of lipids in human plasma. Journal of lipid research. 2010; 51:3299–3305. [PubMed: 20671299]
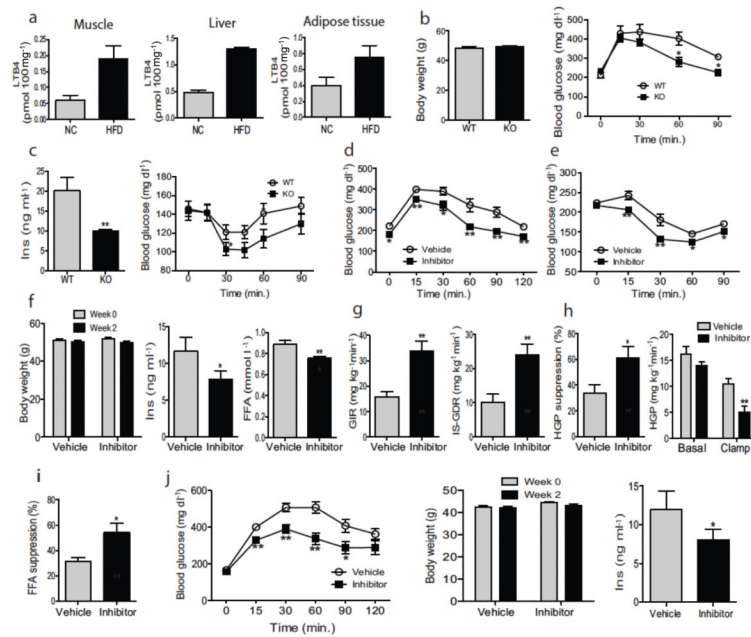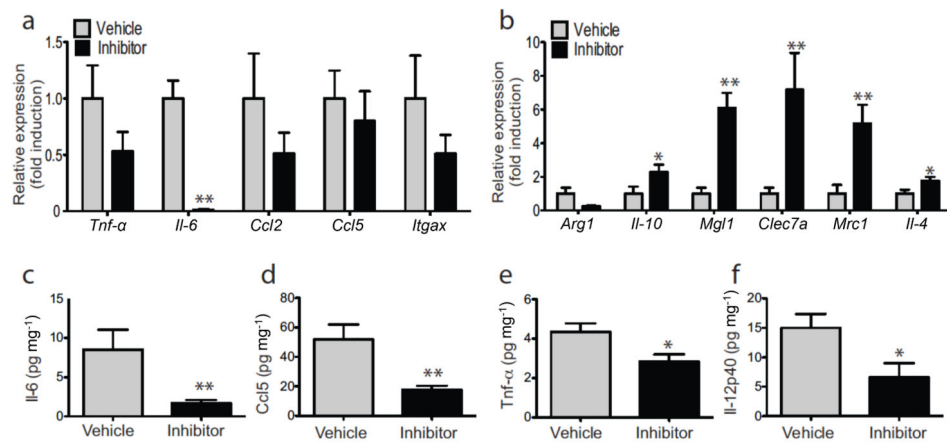
Figure 1.
Inhibition of Ltb4r1 led to an insulin sensitive phenotype. (**a**) LTB4 levels in muscle, liver and Epi-WAT of normal chow or HFD mice. (**b**) Body weight and GTT of WT and Ltb4r1 KO mice on HFD. (**c**) Serum insulin level and ITT of WT and Ltb4r1 KO mice. (**d**) GTT of HFD mice treated with vehicle or Ltb4r1 inhibitor. (**e**) ITT of HFD mice treated with vehicle or Ltb4r1 inhibitor. (**f**) Body weight, serum insulin and FFA level of HFD mice treated with vehicle or Ltb4r1 inhibitor. (**g**) Glucose infusion rate (GIR), Insulin stimulated glucose disposal rate (IS–GDR). (**h**) Hepatic glucose production (HGP) suppression, and HGP. (**i**) Free fatty acid (FFA) suppression in the glucose clamp studies in HFD mice treated with vehicle or Ltb4r1 inhibitor. (**j**) GTT, body weight, and serum insulin level in *ob/ob* mice treated with vehicle or Ltb4r1 inhibitor. Data were analyzed by two-way ANOVA followed by Bonferroni post tests. Values are expressed as mean ± s.e.m. n=6 in a and f-i. n=10 in **b-e** and **j**. * *P*<0.05, ** *P*<0.01 for vehicle versus treatment, or KO versus WT.
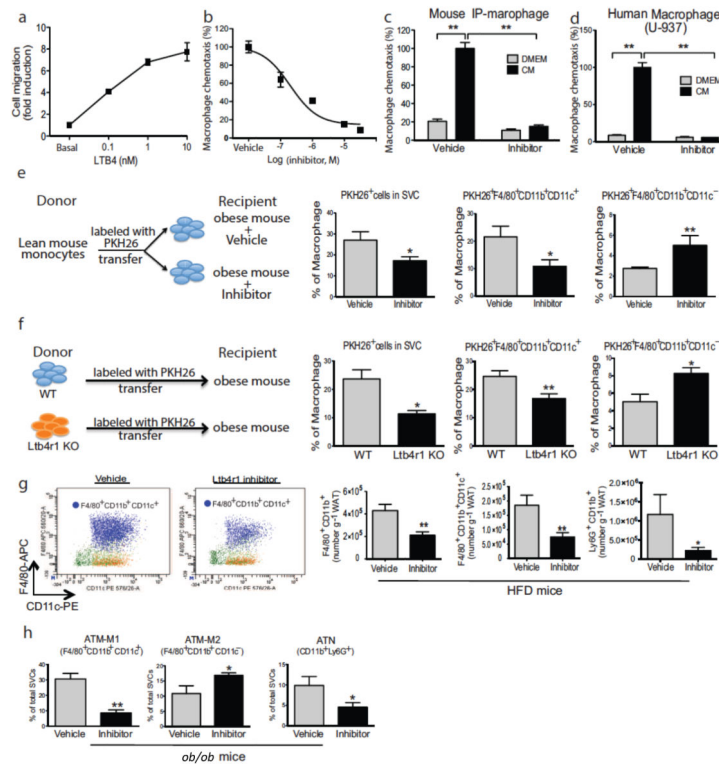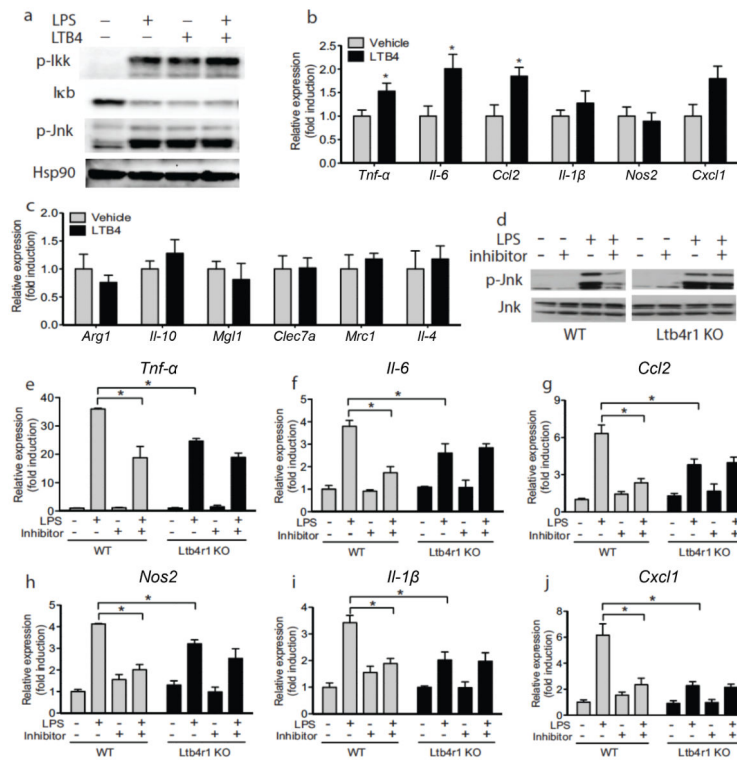
Figure 2.
Ltb4r1 inhibitor blocked macrophage chemotaxis both *in vitro* and *in vivo*. (**a**) Effect of LTB4 on macrophage chemotaxis. (**b**) Effect of Ltb4r1 inhibitor (100 nM) on LTB4 induced chemotaxis. (**c**) Effect of Ltb4r1 inhibitor on 3T3-L1 CM induced chemotaxis of IP-MACs. (**d**) Effect of Ltb4r1 inhibitor on 3T3-L1 CM induced chemotaxis in human macrophages. (**e**) *In vivo* tracking of PKH26 positive monocytes in obese WT mice treated with vehicle or Ltb4r1 inhibitor. (**f**) *In vivo* tracking of monocytes from WT or Ltb4r1 KO mice into obese WT mice. (**g**) FACS analysis of macrophages in Epi-WAT from HFD mice treated with vehicle or Ltb4r1 inhibitor. (**h**) FACS analysis of macrophages in Epi-WAT from *ob/ob* treated with vehicle or Ltb4r1 inhibitor. (**i**) FACS analysis of neutrophils in Epi-WAT of HFD mice treated with vehicle or Ltb4r1 inhibitor. Data were analyzed by two-way ANOVA followed by Bonferroni post tests. Values are expressed as mean ± s.e.m. n=4 in **a–b** and **e–f**. n=6 in **c–d** and **g–h**. * $P<0.05$, ** $P<0.01$ for vehicle versus treatment, or KO versus WT. FACS gating strategy was described in supplemental Figure 4.
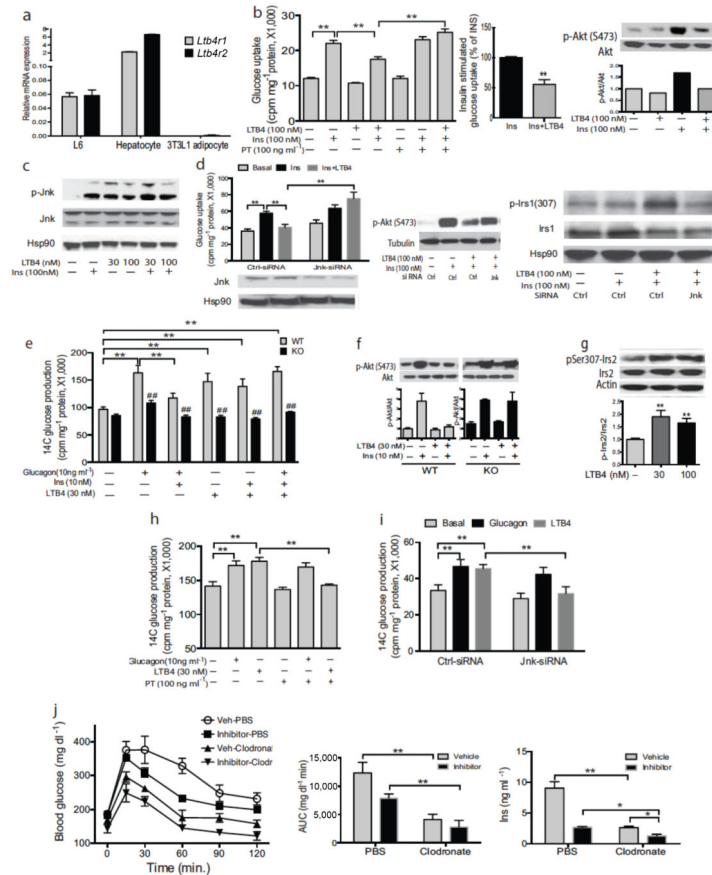
Figure 3.
Ltb4r1 inhibitor improved Epi-WAT inflammation in HFD mice. (**a**) Relative mRNA level of inflammatory cytokines in Epi-WAT of HFD mice treated with vehicle or Ltb4r1 inhibitor. (**b**) Relative mRNA level of anti-inflammatory cytokines in Epi-WAT of HFD mice treated with vehicle or Ltb4r1 inhibitor. (**c**) Serum Il-6, (**d**) Rantes, (**e**) Tnf-α and (**f**) Il-12p40 levels in HFD mice treated with vehicle or Ltb4r1 inhibitor. Data were analyzed by two-way ANOVA followed by Bonferroni post tests. Values are expressed as mean ± s.e.m. n=6 in **a-f**. * $P<0.05$, ** $P<0.01$ for vehicle versus treatment, or KO versus WT.
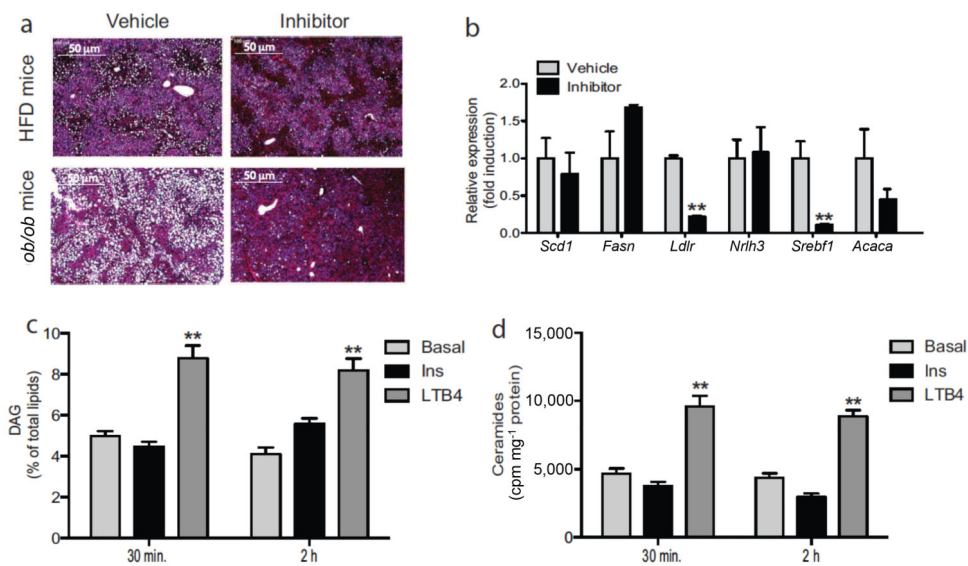
Figure 4.
Ltb4r1 inhibitor ameliorates inflammation. (**a**) p-Ikkβ IκB and p-Jnk in IP-MACs after LPS or LTB4 stimulation. Q-PCR analysis of pro-inflammatory M1-like (**b**) or anti–inflammatory M2-like (**c**) genes in IP-MACs after LTB4 stimulation. (**d**) The effect of Ltb4r1 inhibitor (100 nM) on p-Jnk induced by LPS in IP-MACs. Effect of Ltb4r1 inhibitor (100 nM) on *Tnf-α* **e**), *Il6* (**f**), *Ccl2* (**g**), *Nos2* (**h**), *Il1β* (**i**), and *Cxcl1* (**j**) in IP-MAC from WT or Ltb4r1 KO mice after LPS stimulation by q-PCR analysis. IP-MACs were treated with LTB4 (100 nM) for 45 min or Ltb4r1 inhibitor (100 nM) for 1 hour, followed by LPS (100 ng ml^{-1}) treatment for 15 min in **a** and **d**, and 6 hours in **b-c** and **e-j**. Data were analyzed by two-way ANOVA followed by Bonferroni post tests. Values are expressed as mean ± s.e.m. n=6 in **b-c** and **e-j**. Western blot data are represented of more than 3 independent experiments. * *P*<0.05, ** *P*<0.01 for vehicle versus treatment, or KO versus WT.

Figure 5.
LTB4 directly induces insulin resistance in myocytes and hepatocytes. (**a**) Relative mRNA level of Ltb4r1 and Ltb4r2 in L6 cells, primary hepatocytes and 3T3-L1 cells. (**b**) Effect of LTB4 and the Gαi inhibitor PT on insulin stimulated glucose uptake and p-Akt in L6 cells. (**c**) Effect of LTB4 and PT (100 ng ml^{-1}) on p-Jnk in L6 cells. (**d**) Effect of LTB4 and Jnk siRNA on insulin stimulated glucose uptake, p-Akt and p-Irs1 (Ser307) in L6 cells. (**e**) Effect of LTB4, glucagon and insulin on glucose output in WT and Ltb4r1 KO primary hepatocytes. (**f**) Effect of LTB4 on p-Akt in WT and Ltb4r1 KO primary hepatocyte. (**g**) Effect of LTB4 on p-Irs2 (Ser307) in primary hepatocytes. (**h**) Effect of PT (100 ng ml^{-1}) on glucose output in primary hepatocytes. (**i**) Effect of Jnk siRNA on glucose output in primary hepatocytes. (**j**) Effect of clodronate on glucose tolerance, AUC of glucose tolerance test, and insulin concentration in vehicle or Ltb4r1 inhibitor treated mice. Data were analyzed by two-way ANOVA followed by Bonferroni post tests. Values are expressed as mean ± s.e.m. n=6 in **a-b**, **d-e**, and **h-j**. Western blot data are represented of more than 3 independent experiments. * $P<0.05$, ** $P<0.01$, ## $P<0.01$ for KO versus WT.

Figure 6.
Ltb4r1 inhibitor improves hepatic steatosis. (**a**) HE staining of liver from HFD or *ob/ob* mice treated with vehicle or Ltb4r1 inhibitor. The scale bar indicates 50 μm. (**b**) Relative mRNA levels of lipogenesis/gluconeogenesis genes in liver of HFD mice treated with vehicle or Ltb4r1 inhibitor. (**c**) Effect of LTB4 on DAG content in hepatocytes. (**d**) Effect of LTB4 on ceramides content in hepatocytes. Data were analyzed by two-way ANOVA followed by Bonferroni post tests. Values are expressed as mean ± s.e.m. n=6 in **a-d**. * $P<0.05$, ** $P<0.01$ for vehicle versus treatment, or KO versus WT.